Westinghouse Astronuclear Laboratory

FRACTURE TOUGHNESS OF BERYLLIUM

UNCLASSIFIED NERVA RESEARCH
AND DEVELOPMENT REPORT.

DISCLAIMER

DISCLAIMER

Portions of this document may be illegible in electronic image products. Images are produced from the best available original document.

FRACTURE TOUGHNESS OF BERYLLIUM

by

D. L. Harrod

T. F. Hengstenberg

M. J. Manjoine

UNCLASSIFIED NERVA RESEARCH

AND DEVELOPMENT REPORT.

APPROVED BY:

E. T. C. Layland

E. L. Layland, Manager
Materials Engineering and Specifications

R. T. Begley
Mgr., Materials Science Group

D. E. Thomas, Engineering Manager
Systems and Technology

INFORMATION CATEGORY

unclassified

E. L. Layland   7/6/67

AUTHORIZED CLASSIFIER   DATE

ABSTRACT

The opening mode plane strain fracture toughness of vacuum hot pressed S-200 grade beryllium was determined in the temperature range -320°F to 500°F. Two different test specimen designs were employed, and a number of other variables were investigated to a limited extent. The temperature dependence of fracture toughness was found to be approximately linear between -320°F and room temperature. Fracture toughness was nearly isotropic, and was not dependent upon loading rate for crosshead speeds up to 2 in/min. Heat treatments were found to have a pronounced effect on fracture toughness. Fractographic observations failed to reveal any correlation between fracture toughness and the various test variables, including the response to heat treatment and the effect of test temperature.

**Astronuclear
Laboratory**

CONTENTS

INTRODUCTION

Intuitively it would seem that the methods of fracture mechanics should be eminently applicable to the design and analysis of beryllium structural components. Yet, in spite of the technological interest in beryllium and its brittleness, no fracture toughness data on beryllium have appeared in the open literature. Aside from the present work, the only other work on beryllium, of which the authors are aware, is that being done by Harris and Dunegan at the Lawrence Radiation Laboratory (Ref. 1).

The data presented here were obtained in connection with the design and analysis of beryllium neutron reflectors in the NERVA engine. The main objective was to determine the opening mode plane strain fracture toughness, K_{IC}, at temperatures in the range $-320°F$ to room temperature. However, other variables were also considered, such as test specimen design, effects of neutron irradiation[*], specimen orientation (anisotropy), loading rate, heat treatment, and higher test temperatures.

EXPERIMENTAL PROCEDURES

In anticipation of greater activity in fracture mechanics studies on beryllium in the near future, and recognizing the lack of experience in fracture toughness testing of beryllium, as well as the importance of material characterization, it was judged warranted to discuss the experimental procedures in some detail. Specifically, the aim here is to make quite clear how the tests were run, how the data were calculated, and the nature of the beryllium metal that was studied.

SPECIMEN DESIGN AND ANALYSIS

The major problem to be resolved at the outset was that of selecting a suitable test specimen. In principle, any number of test specimens might be used – all of which should give the same result. Usually, however, experimental problems exist which are peculiar to each material

---

[*]These tests are still in progress and will be reported upon later.

and specimen design. It was finally decided to use two specimens, in part to provide an internal check on the results and in part to circumvent certain experimental problems. These two specimens are designated, herein, as (1) the WOL (wedge opening loading) specimen[*] and (2) the DCB (double cantilever beam) specimen. The WOL specimen is particularly well suited to our studies on neutron irradiation effects in that the specimen is compact and the test is simple and easy to perform. Also, a well established analytical expression for the stress intensity factor, K_I, exists. The normal practice is to pre-crack the WOL specimen by a fatigue method. However, it was anticipated that this might be difficult to achieve with beryllium, or at least it might require a sizeable experimental effort in itself. Assuming that the machined notch could not be readily extended by fatigue, the question immediately arose as to whether or not the results obtained with the machined notch would be the same as those that would have been obtained with a natural crack. It was mainly because of this point that the DCB specimen was included in the program. With the DCB specimen, natural cracks can be formed if the specimen is suitably dimensioned.

WOL SPECIMEN

The configuration of the WOL specimen is shown in Figure 1. The K-calibration, i.e., relation between the stress intensity factor K_I, the applied load P, and the specimen dimensions has been determined for this specimen by W. K. Wilson, (Ref. 2) and is

$$\text{(Eq. 1)} \quad K_I = \frac{P}{\sqrt{a} \; B} \left[-5.605 + 61.27 \left(\frac{a}{w}\right) - 141.08 \left(\frac{a}{w}\right)^2 + 142.80 \left(\frac{a}{w}\right)^3 \right]$$

This expression is valid for $H/W = 0.444$ and for a/w in the range $0.26 \leq a/w \leq 0.62$. For geometrically similar specimens but of other dimensions, other expressions for K_I exist which differ from Eq. 1 in the value of the polynomial enclosed in brackets. For details on these other specimens, stress analyses, etc., see References 3 and 4.

---

[*]The WOL specimen was originally designed by M. J. Manjoine of Westinghouse, and is sometimes called the Manjoine specimen.

a_0 = 0.500"

W = 1.125"

H = 0.500"

B = 1.000"

611735-2B
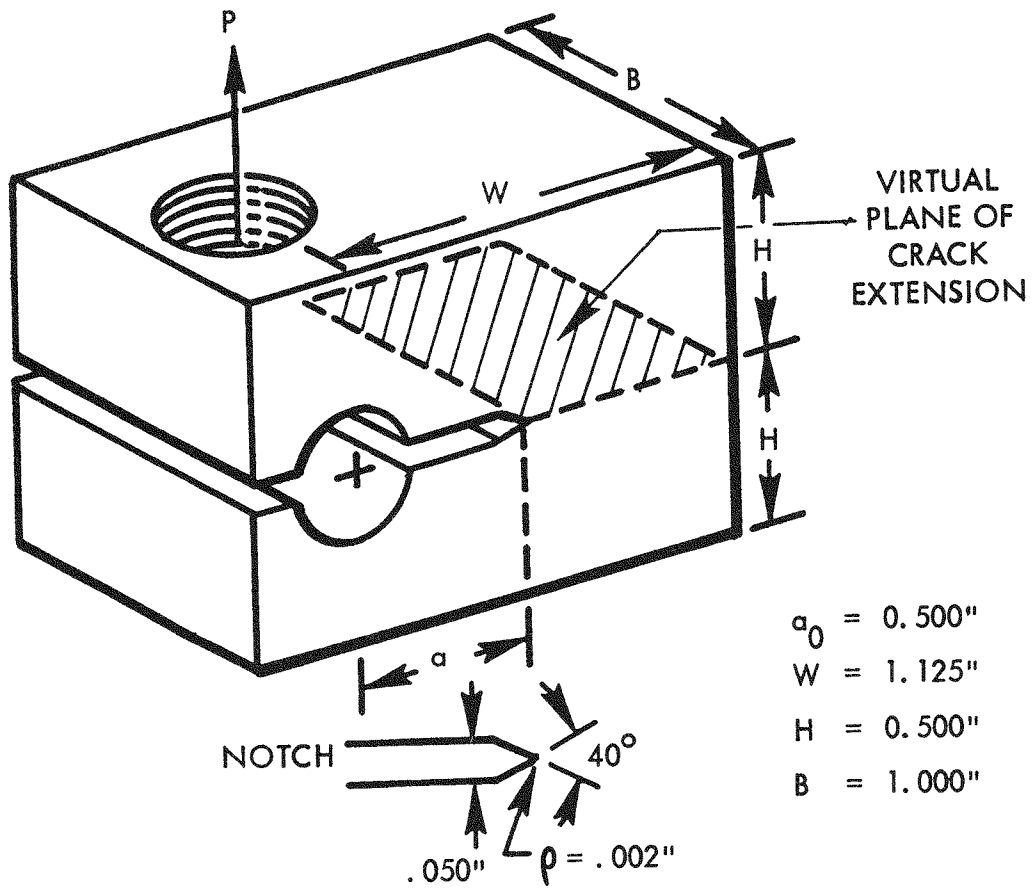
FIGURE 1.   Configuration of WOL Specimen

3

Data analysis can be simplified if Eq. 1 is rewritten as

(Eq. 2)
$$K_I = \frac{P \, C^*}{\sqrt{a} \; B}$$

where C^* is the polynomial in a/w of Eq. 1. The value of C^* has been plotted as a function of a/w in Figure 2. Thus, to determine the fracture toughness, K_{IC}, i. e., the value of K_I at the onset of unstable crack propagation, it is only necessary to measure the load P and crack length "a" at the instant of instability; C^* is obtained graphically and B is known.

All attempts at pre-cracking the WOL specimen by tension-tension fatigue were unsuccessful. Hence, the specimens were all tested using the machined notches. Since no "pop-in" phenomena nor slow crack growth were observed in any of the tests on beryllium with this specimen, K_{IC} values were calculated using the maximum load and the initial crack (notch) length. The values of K_{IC}, however, were corrected to allow for the plastic deformation occurring at the tip of the notch according to the customary procedure established by Irwin (Ref. 5). This correction was made in the following manner: The extent of the plastic zone, r, was calculated from the expression,

(Eq. 3)
$$r = \frac{1}{6\pi} \left(\frac{K'}{\sigma_Y} \right)^2$$

where σ_y is the 0.2% offset yield strength, and K' is calculated using the initial notch length, a_o, and the associated initial value of C^*. This value of r is then added to a_o to give an adjusted crack length $a = a_o + r$. This gives new values of a/w and C^* (See Figure 2) which are used to calculate K_{IC}, i. e.,

(Eq. 4)
$$K_{IC} = \frac{P \text{ max. load} \times C^* \text{ adjusted}}{\sqrt{a_o + r} \times B}$$

This correction amounted to increasing the initial value of K_{IC} (K') by about 25 to 1500 psi $\sqrt{\text{inch}}$. The values of r ranged from about 0.002 to about 0.03 inch.

FIGURE 2. Numerical Constant C* of Eq. 2 vs. a/w

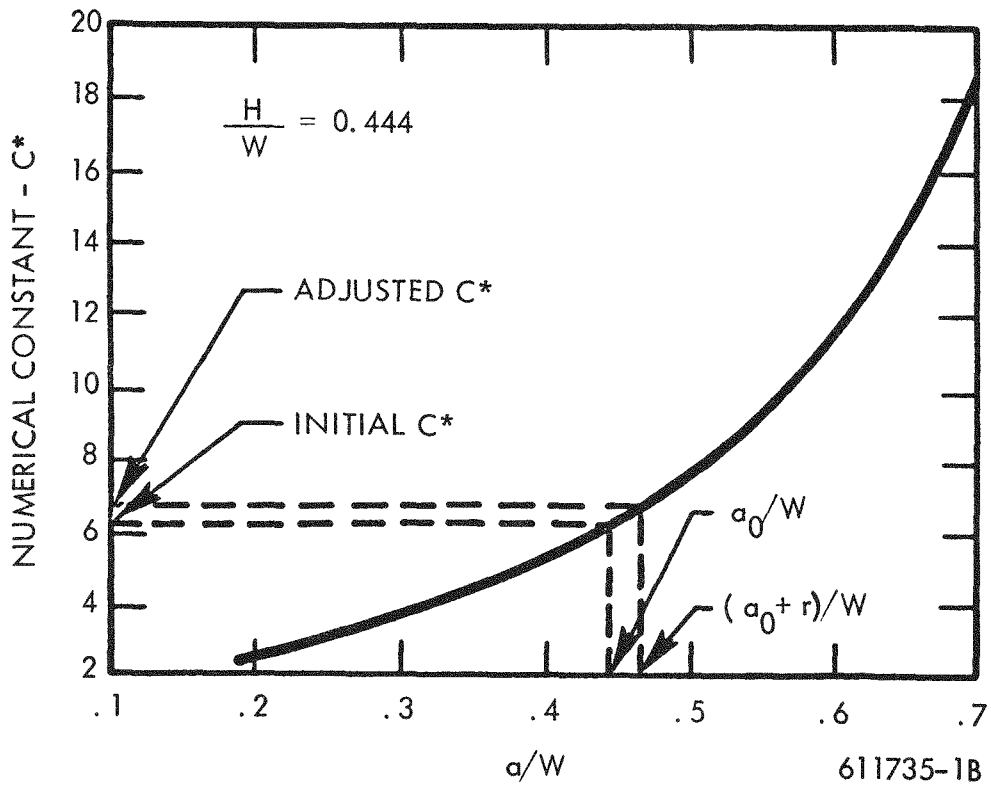The WOL specimens were tested in an Instron testing machine. An example of the type of load-deflection curves obtained using a clip-on compliance gage is shown in Figure 3. Some deviation from linearity was observed in all the tests.

DCB SPECIMEN

The configuration of the DCB specimen is shown in Figure 4. The design and analysis of this specimen has been described by Ripling, Mostovoy, and Patrick (Ref. 6), and also by Mostovoy, Crosley, and Ripling (Ref. 7). Like the WOL specimen, crack-line loading rather than remotely applied loading is employed. With the DCB specimen, the crack-extension force, G_I, decreases with increasing crack length, and this can lead to stable crack extension or crack arrest. Thus, the applied crack-extension force (strain energy release rate) G_I increases with increasing applied load P. When the applied G_I reaches the critical value G_{IC} for the material, the crack propagates. As the crack runs, the applied G_I decreases, and the crack arrests when G_I drops below G_{IC}. The load is then again increased and the process repeated. A large number (12 to 40 for our beryllium specimens) of crack initiations and arrests may be observed on one test specimen. Each initiation gives an independent measurement of G_{IC} and each arrest gives a measurement of the strain energy release rate at crack arrest, G_a.

The strain energy release rate G_I is given by

$$(Eq.\ 5) \qquad\qquad G_I = \frac{P^2}{2b_n} \frac{dC}{da}$$

where P is the applied load, b_n is the specimen width at the base of the side grooves (which confine the crack to the desired plane) and dC/da is the rate of change of compliance C with crack length a. To evaluate dC/da, Ripling et. al. have shown that the strength of materials solution for the compliance (inches deflection per pound of load, measured at the point of load application) is given by
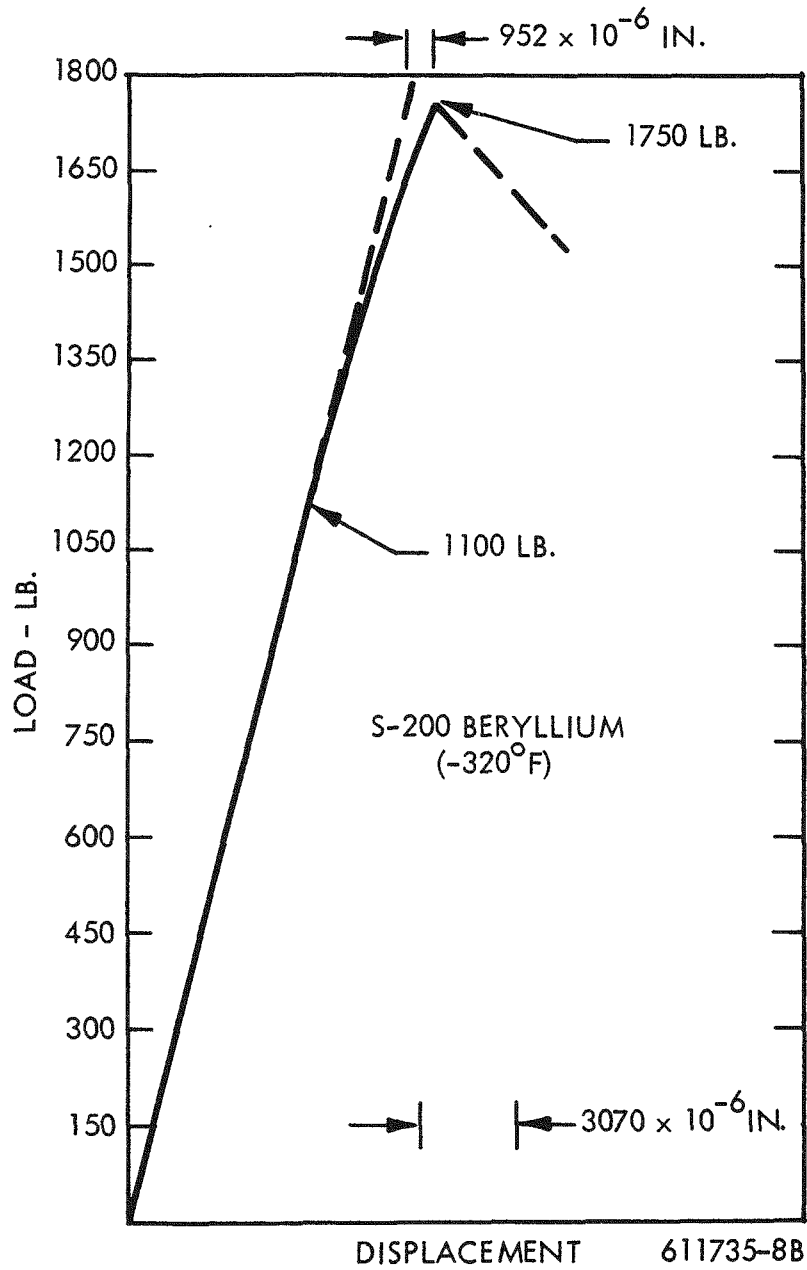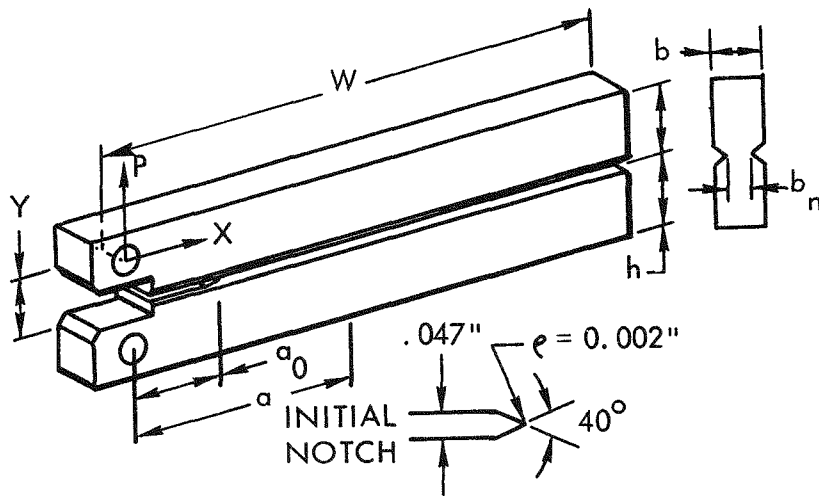
FIGURE 3. Example of Load-Deflection Curves Obtained with WOL Specimens

7

W = 7.0"
b = 0.250"
b_n = 0.130"
h = 0.50"
a_0 = 1.0"

P = LOAD
Y = DISPLACEMENT

611735-5B

FIGURE 4.   Configuration of DCB Specimen

8

(Eq. 6) $\quad C = \dfrac{24}{Eb} \displaystyle\int_o^a \dfrac{x^2}{h^3}\, dx + \dfrac{6(1+\nu)}{Eb} \displaystyle\int_o^a \dfrac{1}{h}\, dx + \text{Correction}$

$\qquad\qquad\qquad$ (Bending) $\qquad\qquad$ (Shear) $\qquad\qquad$ (Rotation)

In this expression, E is Young's Modulus, ν is Poisson's ratio, and the other symbols are defined in Figure 4. Experimentally, Ripling et. al. found that the correction for the rotation contribution to the compliance could be made by replacing the crack length "a" in the bending contribution by $a + \bar{a}$, where $\bar{a} \approx 0.6h$. With this substitution, integration of Eq. 6 gives,

(Eq. 7) $\qquad C = \dfrac{8}{Ebh^3}(a+\bar{a})^3 + \dfrac{6(1+\nu)}{Ebh}\, a$

After substitution of Eq. 7 into Eq. 5 and carrying out the differentiation, the expression for the strain energy release rate for the DCB specimen becomes,

(Eq. 8) $\qquad G_I = \left[\dfrac{24(a + 0.6h)^2}{Ebh^3} + \dfrac{6(1+\nu)}{Ebh}\right]\dfrac{P^2}{2b_n}$

Thus, to measure G_{IC} it is only necessary to measure P and "a" at instability. Since it is difficult to measure the crack length, even in room temperature tests, a convenient recourse is to establish a compliance-crack length calibration. From Eq. 7, for example, if the compliance is measured for each loading, the crack length can be calculated.

Compliance-crack length calibration curves for the DCB specimen are shown in Figure 5. The curves labeled "theoretical" were calculated using Eq. 7. The curve labeled "experimental" was experimentally determined using a saw-slotted specimen which had a beam height h_s = 0.47". Comparison of Curve 1 with Curve 2, therefore, shows the difference between the experimental and theoretical "C versus a" calibration curves. The experimental curve is
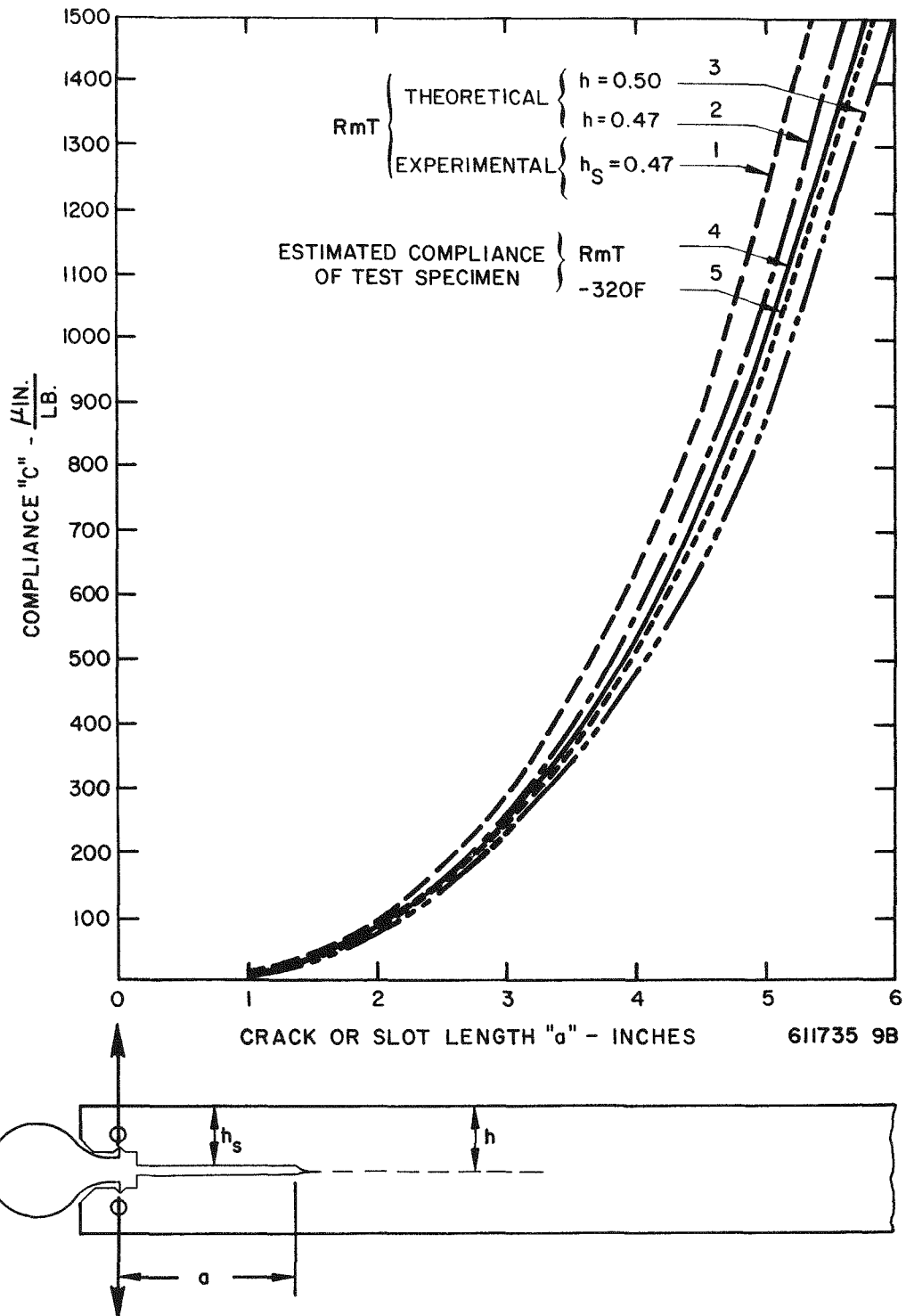
FIGURE 5.   Compliance vs. Crack Length Calibration Curves for Beryllium DCB Specimen

taken to be the correct curve. However, this curve was determined for h = 0.47", whereas for a cracked specimen h = 0.50". This curve, Curve 3, was then adjusted (to the left) by an amount equal to the difference between Curves 1 and 2. This, then, gives Curve 4, which is the estimated compliance of the actual test specimens. Curve 5 was obtained from Curve 4 by adjusting for the change in elastic modulus with test temperature.

The DCB specimens were tested in a specially built load frame which had a very small compliance compared with that of the test specimen. The loading rate was generally in the range 50 to 400μ in/sec. An example of the load-deflection curves obtained while testing one specimen is shown in Figure 6. For the first loading, G_{IC} was calculated from Eq. 8 using the maximum load and a_o = 1.0", the initial notch length. For the fifth loading, for example, the compliance was 66.5μ in/lb, and from the compliance calibration curve, the crack length would had to have been a = 1.7". Thus, for the fifth loading, G_{IC} was calculated using the maximum load for the fifth loading and a = 1.7". The G_{IC} values for the other curves were similarly calculated. Actually, as suggested by Ripling, Eq. 8 was solved graphically by means of a plot like that shown in Figure 7. The crack arrests values, G_a, were calculated in a similar manner, except that the crack length corresponding to a given arrest load was determined from the compliance of the subsequent loading curve.

MATERIAL CHARACTERIZATION

The test specimens all came from the same vacuum hot pressed (VHP) beryllium block (Brush Beryllium structural grade S-200). Figure 8 shows the size of the pressing and the location and orientation of the test specimens. The composition of the pressing was as follows:

Chemical Analysis (wt. %) of Pressing No. 3840

Be	BeO	C	Fe	Al	Mg	Si	Mn
98.2	1.70	0.12	0.14	0.08	0.005	0.03	0.01
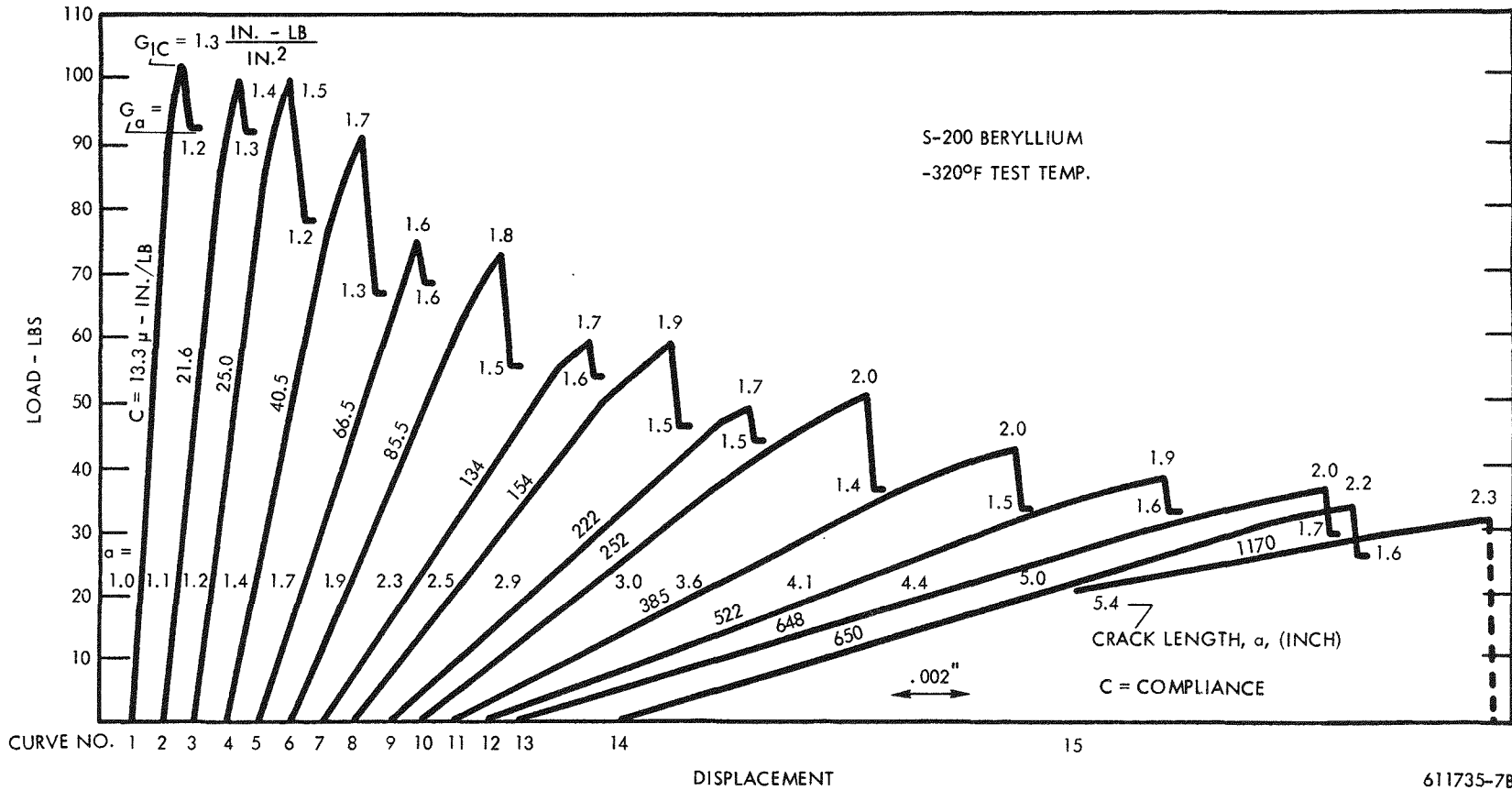
FIGURE 6. Example of Load-Deflection Curves Obtained with one DCB Specimen. Values of Crack Length a, Compliance C, G_a for Crack Arrest, and G_{IC} for Rapid Crack Propagation are Shown on the Curves.

611735-7B

12
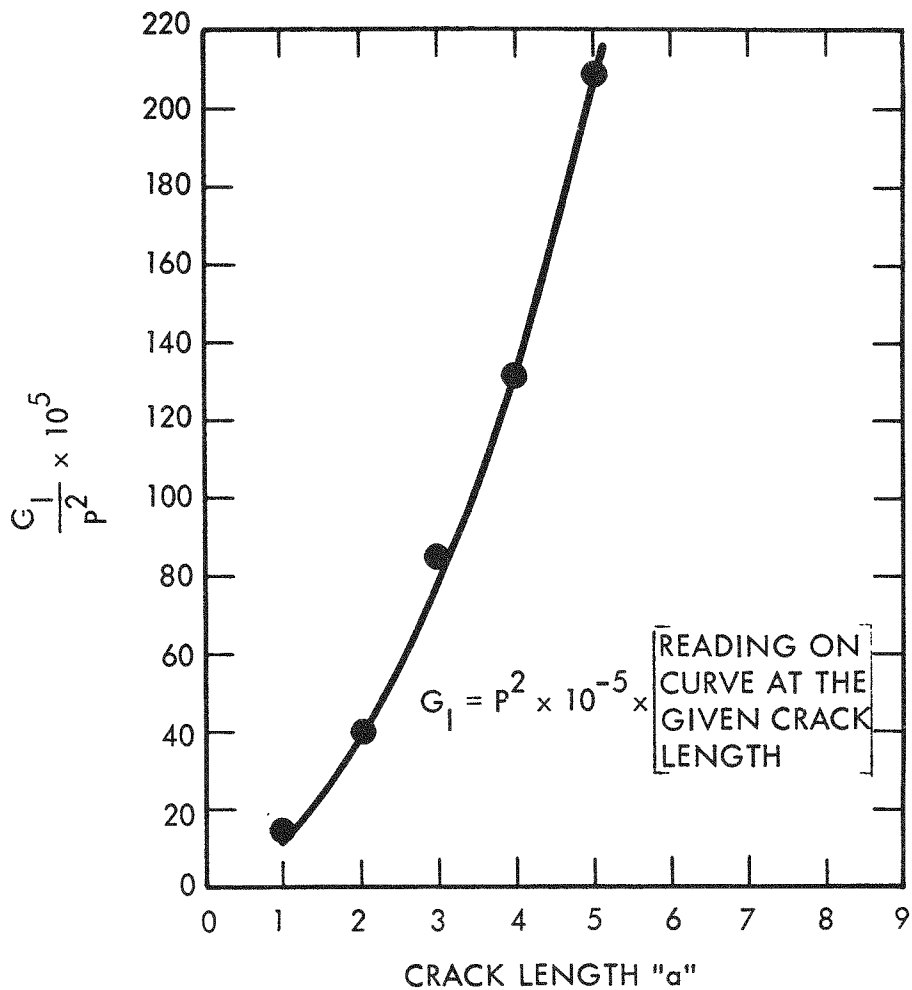
FIGURE 7. Graphical Representation of Eq. 8 of Text. The Load P is Measured and the Crack Length "a" is Obtained from the Measured Compliance "C" per Figure 5. G_{IC} or G_a are Obtained from the Above Graph. The Points (Solid Circles) are Based upon the Analysis by Hoagland et al. (See Discussion Section of Text).

(S-200 GRADE)

VHP BERYLLIUM BLOCK: PRESSING NO. 3840
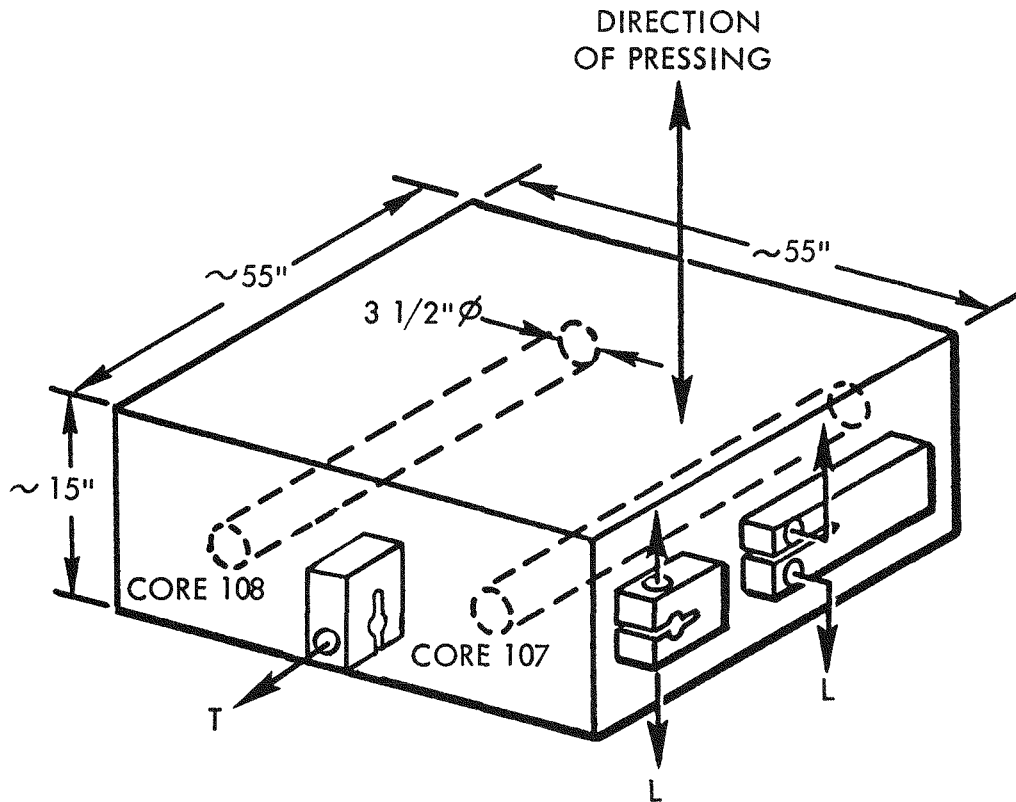
TEST MATERIAL CAME FROM TREPANNED CYLINDERS, CORES 107 AND 108

SPECIMEN ORIENTATION: L (LONGITUDINAL) APPLIED LOAD P II DIR. OF PRESSING
T (TRANSVERSE) APPLIED LOAD P ⊥ DIR. OF PRESSING

ALL L-SPECIMENS (WOL AND DCB) CAME FROM CORE 107

ALL T-SPECIMENS (WOL ONLY) CAME FROM CORE 108

611735-3B

FIGURE 8.   Pressing Size and Location and Orientation of Test Specimens
Within VHP Beryllium Block.

The density of the pressing was 1.86 g/cc, and the results of tensile tests at room temperature were as follows:

Core No.	Orientation	UTS (ksi)	0.2% YS (ksi)	% Elong. in 1"
107	L	44.0	33.3	1.1
108	L	42.5	33.0	1.1
107	T	49.0	33.0	2.1
108	T	50.5	33.7	2.5

For purposes of calculating K_{IC} and G_{IC} values, the following properties were used for all test specimens regardless of their orientation or heat treat condition:

Test Temperature	0.2% YS (ksi)	Poisson's Ratio, ν	Young's Modulus, E (psi)
500°F	30	0.10	41×10^6
75°F	33	0.10	42×10^6
-115°F	33	0.10	42×10^6
-320°F	40	0.10	44×10^6

Throughout this paper, the longitudinal orientation (L) means that the applied load was parallel to the direction of pressing, and the transverse orientation (T) means that the applied load was normal to the direction of pressing. Thus, for a longitudinal specimen, the plane of the crack is in a transverse plane of the pressing, and for a transverse specimen, the crack plane is parallel to the direction of pressing.

It is well established that the properties of commercially pure beryllium are significantly influenced by heat treatment, particularly the high temperature tensile properties. This

response to heat treatment is generally attributed to metallurgical reactions; e. g. , precipitation, due to the presence of impurities such as iron, aluminum, and silicon. Also, as shown by the work of Bonfield and Li (Ref. 8), the microstrain characteristics of beryllium, both the stress required to produce a plastic strain of 10^{-6} and the initial rate of strain hardening, are markedly influenced by thermal treatments. Thus, it was of interest to consider the possible effects of heat treatments on the fracture toughness of beryllium.

The heat treatments used were selected on the basis of known effects of heat treatments on the tensile properties of beryllium (Ref. 9). However, it might be noted that these treatments (listed in the section on test results) did not produce any marked microstructural changes which could be readily detected by metallographic observations. Thus, the same microstructural features were observed in all the test specimens (as-VHP and heat treated conditions). These features are shown in Figure 9. The letters designate different features, but these will not be elaborated upon here except as follows: The letters A and B designate relatively large local areas of high and low concentrations, respectively, of particles and voids. Stringers of voids in grain boundaries are indicated by C. A large isolated inclusion, possibly a carbide, is shown at D, and a conglomeration of inclusions is shown at E. The letter F designates another unidentified phase, perhaps elemental aluminum or silicon or eutectics of these elements with beryllium.

The grain structure and distribution of inclusions can be seen in some photomicrographs presented later. Although there is considerable variation or range of grain sizes, the average grain size of the as-VHP material was about 20 microns, and this average grain size was affected very little by heat treatment.
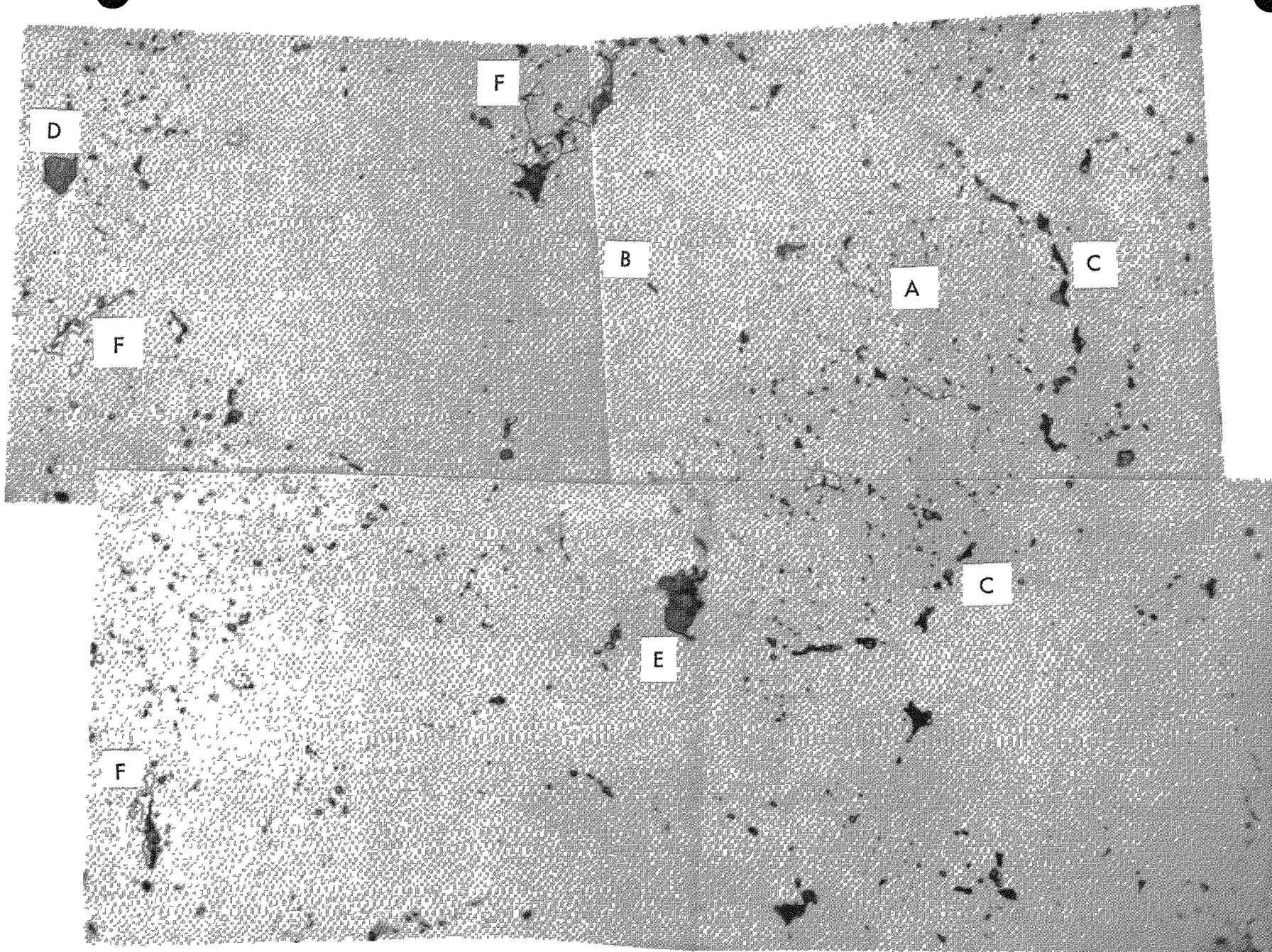
FIGURE 9. Microstructural Features Observed in S-200 Beryllium; VHP + ST 1 hr./1650°F + Aged 120 hrs./932°F (1500X, Bright Field)

RESULTS

The results obtained with the WOL specimen and the DCB specimen are presented separately. Also, some fractographic observations are described. These results will be discussed in more detail in the subsequent section.

WOL SPECIMEN

The K_{IC} data obtained with the WOL specimen are shown in Table 1 and Figure 10. The tests performed at a crosshead speed of 0.005 in/min represent, in a sense, the base-line data; additional variables were investigated in the other tests. For the steploaded tests, one face of the specimens was metallographically polished. The specimen was loaded to a certain load, unloaded, and examined metallographically to assess deformation or cracking at the tip of the notch. This was repeated for a number of increasing loads up to fracture. Several specimens were tested by E. T. Wessel at the Westinghouse Research Laboratory in order to provide a check on experimental procedures. One specimen was chemically etched to remove 4 mils per surface (including the tip of the machined notch), and another specimen was side grooved like the side grooves in the DCB specimen.

The first specimen tested at a fast loading rate (crosshead speed of 2 in/min at -320°F) gave uncertain results in that the recording pen went off the chart on the X-Y recorder. The estimated failure load gave a K_{IC} value of 19 ksi $\sqrt{in}$, or higher. A second test gave a K_{IC} value of 7.3 ksi$\sqrt{in}$. To clarify these results, additional tests at 1 and 2 in/min loading rates were run using a different recording system. These additional tests at both room temperature and -320°F showed no marked effect of the higher loading rate. Thus, the first two tests are listed in Table 1 as being suspect, although no definite evidence exists that the instrumentation malfunctioned.

TABLE 1 – Fracture Toughness, K_{IC}, of S-200 Beryllium – WOL Specimen

| Condition	Crosshead Speed (in/min)	Specimen Orientation Code	K_{IC} (ksi√in)				Comments
			-320°F	-115°F	75°F	500°F	
As-VHP	0.005	T	16.3	19.1	22.4	34.2	Base-line data
	0.005	T	17.2	18.4	25.5		"
	0.005	T			22.4		Step loaded
	0.04	T	16.6				Tested by Wessel
	2.0	T	15.4				High Strain Rate
	0.005	L	15.9	17.7	19.0		Base-line data
	0.005	L	15.7	16.9	21.2		"
	0.005/0.010	L			18.5		Step loaded
	0.005/0.010	L			18.0		Step loaded
	0.005	L			20.4		Chem Etched
	0.005	L			21.3		Side Grooves
	0.04	L	14.6				Tested by Wessel
	1.0	L	15.4		18.8		High Strain Rate
	2.0	L	14.2		18.6		"
	2.0	L	19				" (Test Suspect)
As-VHP	2.0	L	7.3				" (Test Suspect)
ST 1 hr/2100°F	0.005	T	10.7		13.3		As-VHP Plus
ST 2100°F+Aged 73 hr/1385°F	0.005	T	8.3		14.6		Heat Treated
ST 2100°F+Aged 120 hr/932°F	0.005	T	9.6				
As-VHP+Aged 120 Hr/932°F	0.005	T	8.8				
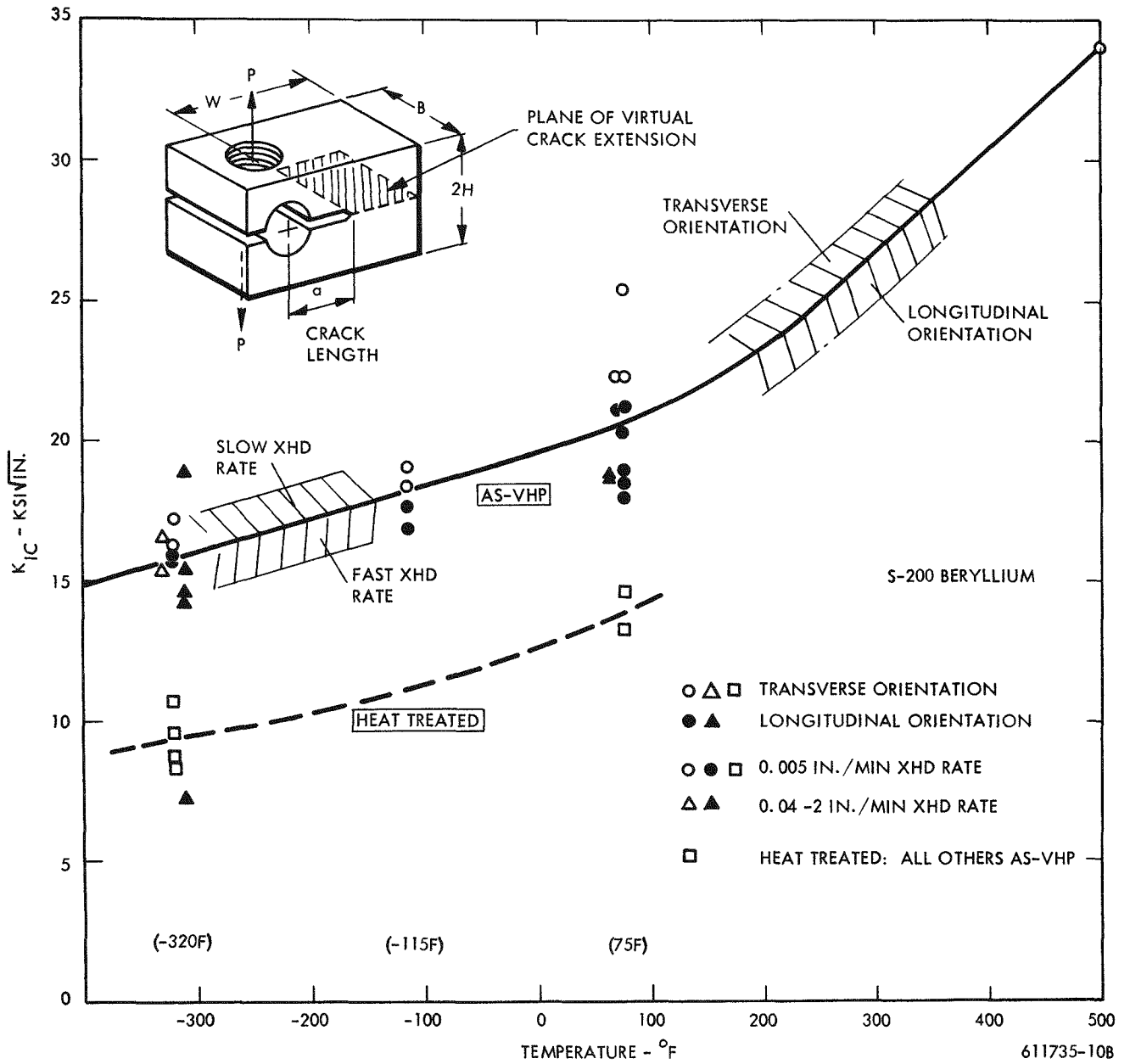
FIGURE 10. Beryllium Fracture Toughness Test Results Obtained with WOL Specimen

As shown in Figure 10, specimen orientation had no pronounced effect on fracture toughness, although the results for the transverse specimens tended to be slightly higher than those of the longitudinal specimens. It might be recalled that the longitudinal and transverse specimens came from opposite sides of a large pressing (Figure 8). Thus, the slight effect observed due to orientation might possibly be due to variation in material from one side of the pressing to the other. In either case, the effect is not large; e. g. , less than 10%.

The results for the chemically etched, side grooved, and step-loaded specimens were about the same as for the as-machined and continuously loaded specimens. Excluding the two tests mentioned above as being suspect, no marked effect of loading rate is evident, although the results for the fast rates appear to be slightly lower than for the slow loading rate.

The heat treated specimens all showed K_{IC} values considerably lower than those of the as-VHP condition. The decrease in K_{IC} due to heat treatment was about 30-40% at both room temperature and at $-320°F$, and for all of the heat treat conditions studied.

DCB SPECIMEN

The results obtained with the DCB specimen are shown in Table 2. It is recalled that in this test it is actually the strain energy release rate, G_I, that is measured; however, for convenience the average test results have been converted to K_{IC} or K_a values, as shown in the right hand column by means of the expression,

$$(\text{Eq. 9}) \qquad K_{IC} = \left[\frac{EG_{IC}}{(1-\nu^2)} \right]^{1/2}$$

All of the data in one horizontal row pertains to one test specimen. Thus, the crack started and stopped anywhere from 12 to more than 40 times in the as-VHP specimens. Exactly the same value of G_{IC}, in principle, should be obtained for each initiation. However, the high and low values obtained on a given specimen differed by as much as a factor of two.

TABLE 2 – Fracture Toughness, G_{IC}, of S-200 Beryllium – DCB Specimen

Condition*	Test Temp. (°F)	Average G_I (in-lb/in²)		ΔG_I, $G_{IC}-G_a$ (in-lb/in²)	Number of Crack Arrests	Range of G_I (in-lb/in²)				Average K_I (ksi √in)	
		G_{IC} (Initiation)	G_a (Arrest)			G_{IC}		G_a		K_{IC} (Initiation)	K_a (Arrest)
						Low	High	Low	High		
As-VHP	-320	2.2	1.8	0.4	19	1.8	2.6	1.5	2.2	9.9	8.9
↑	-320	1.5	1.2	0.3	14	0.9	2.0	0.8	1.6	8.2	7.3
	-320	1.8	1.5	0.3	15	1.3	2.3	1.2	1.7	8.9	8.2
	-115	3.4	2.4	1.0	18	2.3	5.4	1.4	4.9	12.0	10.1
	-115	(See Text)			40						
↓	75	4.7	3.2	1.5	12	3.7	6.3	1.9	4.2	14.1	11.6
As-VHP	75	5.6	4.1	1.5	14	4.7	7.8	3.6	5.2	15.4	13.2
ST 1 hr/2100°F											
ST 1 hr/2100°F+ Aged 120 hr/932°F											
ST 1 hr/1650°F+ Aged 120 hr/932°F											

(The load-deflection curves obtained with these heat treated specimens are presently uninterpretable. For example, see Figure 11. The reason for the difference observed between these curves and those for the as-VHP condition is uncertain.)

* All Specimens in longitudinal orientation

The results obtained with the heat treated specimens were somewhat surprising. It is recalled that heat treatment decreased K_{IC} as determined with the WOL specimen, and a similar result was expected with the DCB specimen. However, the nature of the load-deflection curves for the heat treated DCB specimens differed significantly from those of the as-VHP specimens. The type of load-deflection curves obtained with the as-VHP specimens was previously shown in Figure 6, and an example of the type of curves obtained with the heat treated specimens is shown in Figure 11.

The values of G_{IC} obtained with the first loading curves were about the same as those for the as-VHP condition. However, the maximum loads increased with subsequent loading cycles, while the crack gradually tore down the length of the specimen. In Curve 7 of Figure 11, for example, after first reaching the maximum load, the crack jumped discontinuously, but gradually, at approximately constant load. The load was removed at point A on the curve, otherwise the curve would have continued out to fracture. In all three of the heat treated specimens, one arm of the specimen broke off after the crack had extended to about 3" in length due to the high bending moment developed.

One of the as-VHP specimens tested at -115°F gave a load-deflection curve somewhat similar to those of the heat treated specimens. Gradual, discontinuous cracking at constant load was not observed, but the maximum loads increased for the first five runs and then gradually decreased. The values of G_{IC} gradually increased (but not regularly) from 2.4 to about 9 in-lb/in^2. The nature of the crack growth in this specimen was similar to that in the heat treated specimens, as shown in Figure 12. It appeared as though the crack grew by tearing across the width of the specimen as illustrated in Figure 12a. Visual examination of this specimen reveals a number of points along the fractured surface which appear to be points where the crack arrested (or initiated). Some of these points are marked A in Figure 12b. However, no one-to-one correlation between these points and the actual positions of crack arrest exists. From the load-deflection curves, for example, there were more than 40 crack arrests, yet there are not nearly 40 points of the type marked A in the figure. Also, the appearance of the first 3/4" of the fracture is uniform, yet the crack
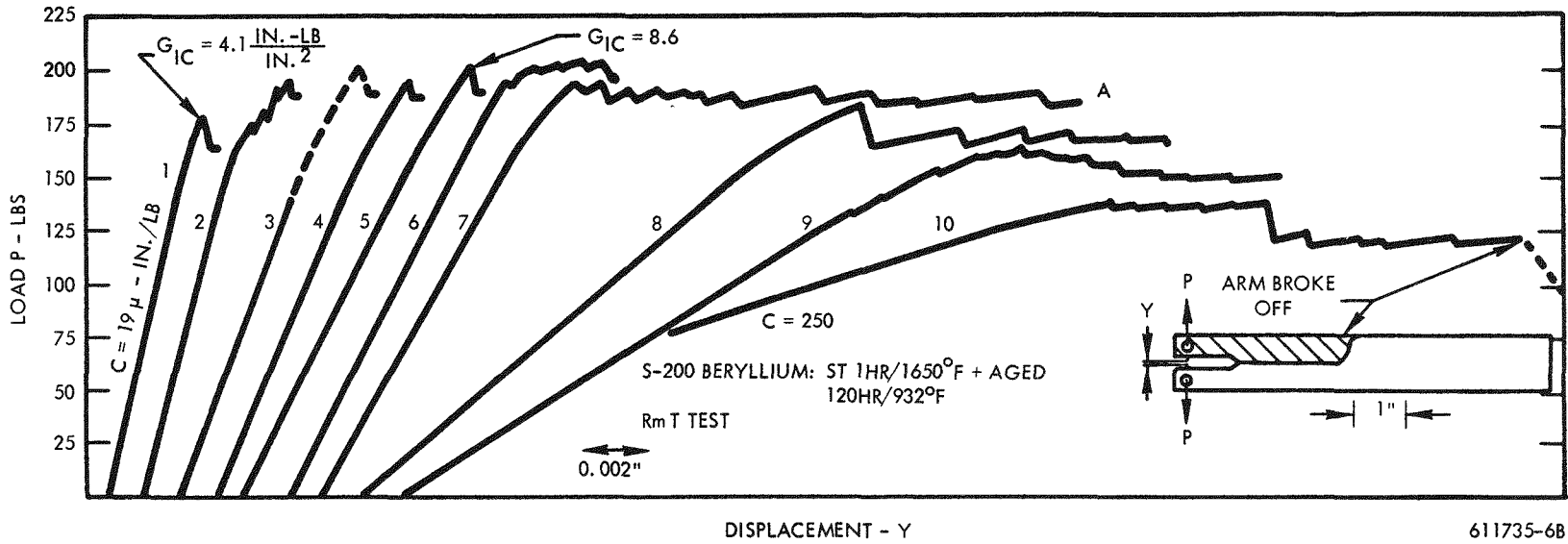
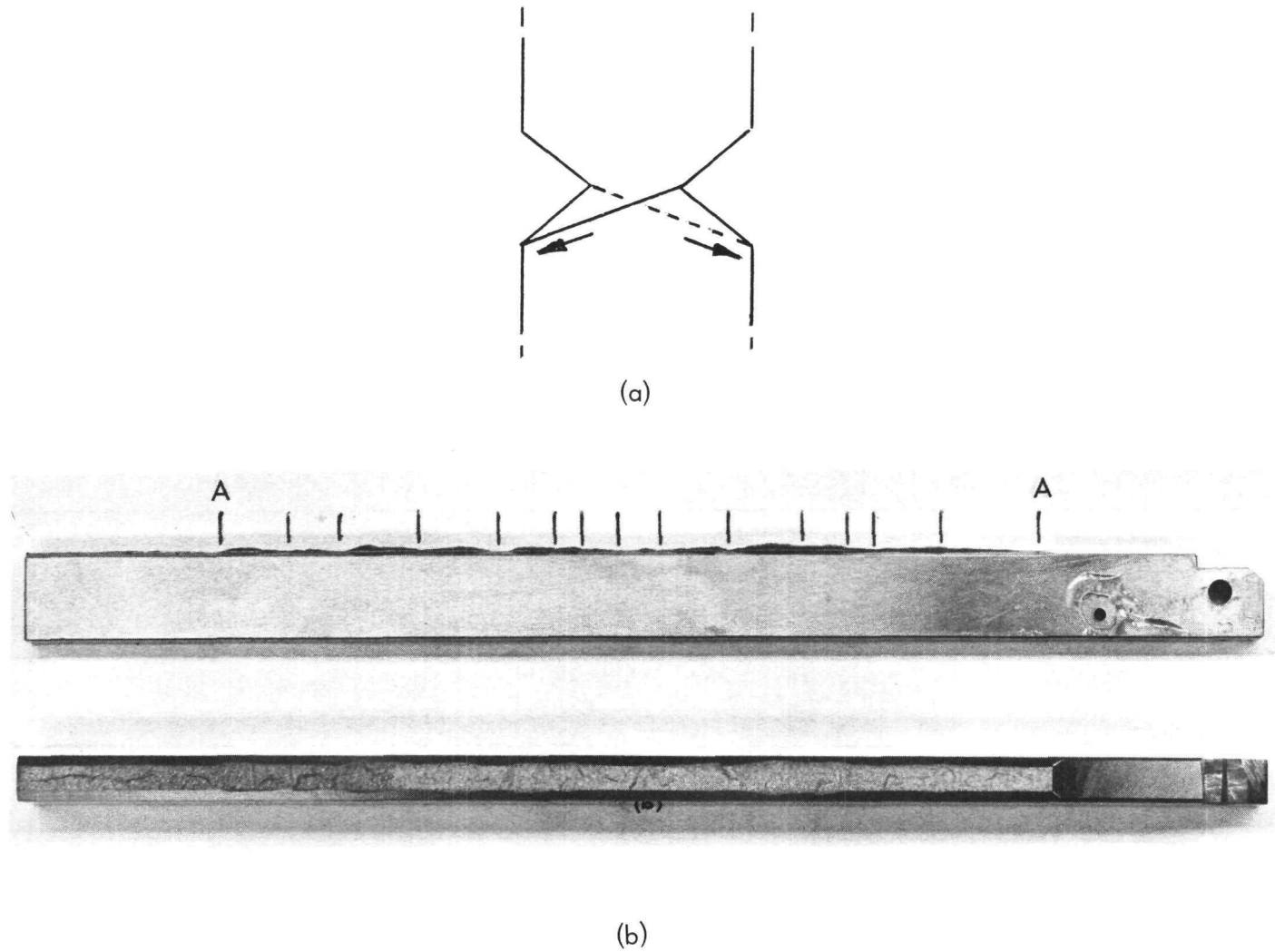FIGURE 11. Example of Load-Deflection Curves Obtained with Heat Treated DCB Specimen

(a)

(b)

FIGURE 12. Illustrating the Nature of Irregular Crack Propagation Observed in One As-VHP
DCB Specimen Tested at -115°F and all Heat Treated DCB Specimens. (a) Schematic
of Tearing Across the Width of the Specimen. (b) Fracture Surfaces.

arrested about ten times along this length.

As a result of the above considerations, the load-deflection curves for the heat treated specimens and one of the as-VHP specimens tested at -115°F are presently uninterpretable, and hence no values for G_{IC} are listed for these specimens in Table 2.

FRACTURE FEATURES

The types of fracture surface profiles observed with the WOL specimen are shown in Figure 13. The transverse specimens tested at 75°F and 500°F generally failed with the crack running to the side of the specimen, as in Figure 13a. Although the nature of the stress field at the tip of the running crack is such that it would tend to cause the crack to run out the side, this was only observed in some of the transverse specimens. This is also consistent with the slight effect of specimen orientation on K_{IC} as previously described. In most cases the crack ran approximately straight across the specimen (Figure 13b), while in some there were various irregularities and humps as in Figure 13c. In all cases there was a flat segment extending from the tip of the notch (normal to the applied load) about 50 mils or more in width, as shown in Figure 13a and 13c. After extending to this depth, the crack path some-times deviated in various directions. This initially short flat segment is not believed to be associated with either the mechanism of crack initiation at a short depth ahead of the notch or with the plastically deformed region associated with the machining operations.

The sequence of micrographs shown in Figure 14 was obtained by step loading a metallo-graphically polished specimen and examining the specimen after each loading. Note the large grain indicated by the arrow in the initial (no load) condition. The small marking in this grain, running normal to the notch axis, may be either a twin or a bend plane. No difference was observed after loading to 1800 and 1850 lbs. At 2000 lbs., the small crack running parallel to the notch axis was observed. This crack grew with increasing load, and formed part of the main fracture path when fracture occurred at 2300 lbs. This, of course, is only an observation on the free surface of the specimen, but it suggests that crack initiation occurred below the root of the notch at a depth considerably greater than the average grain
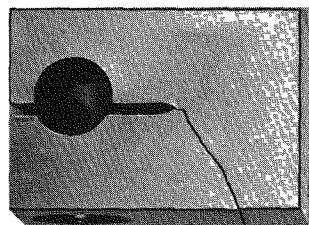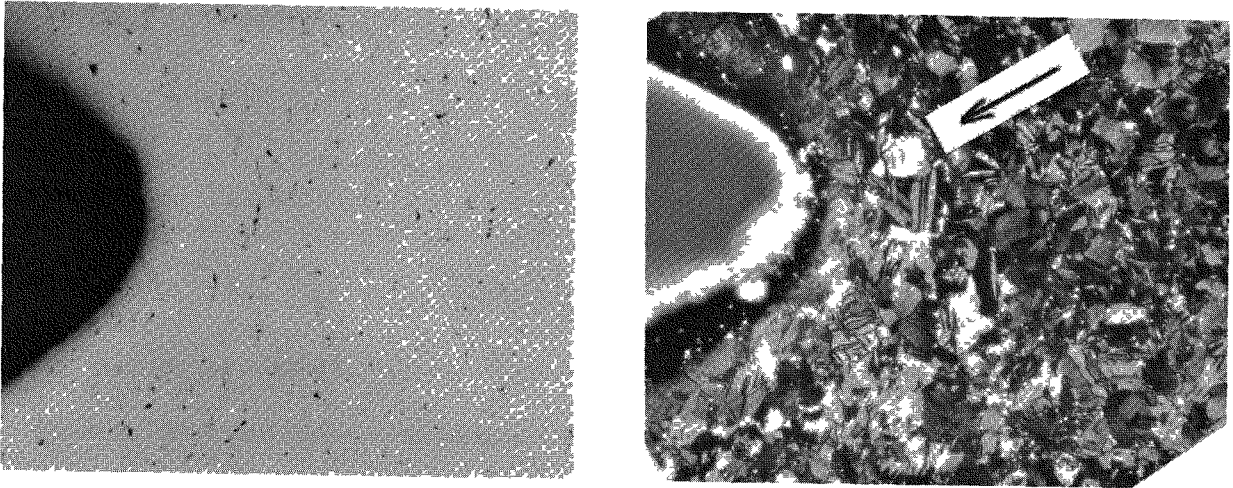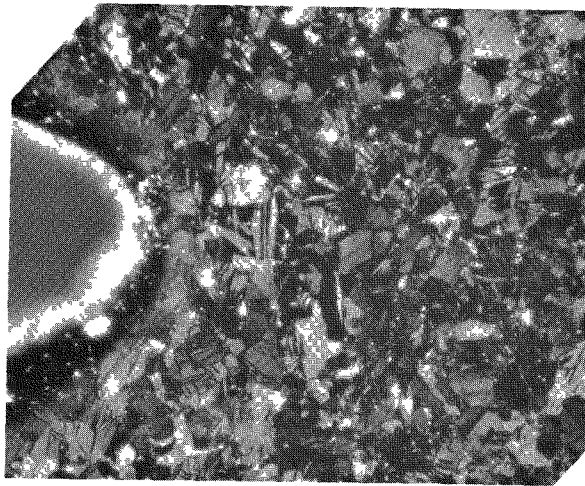
(a)
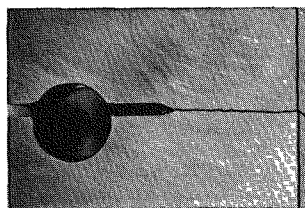
(b)
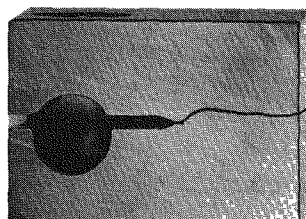
(c)

FIGURE 13. Showing Different Types of Fracture Paths Observed in WOL Specimens
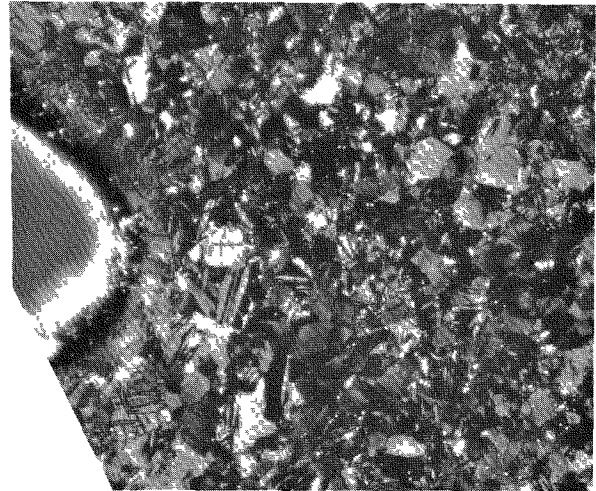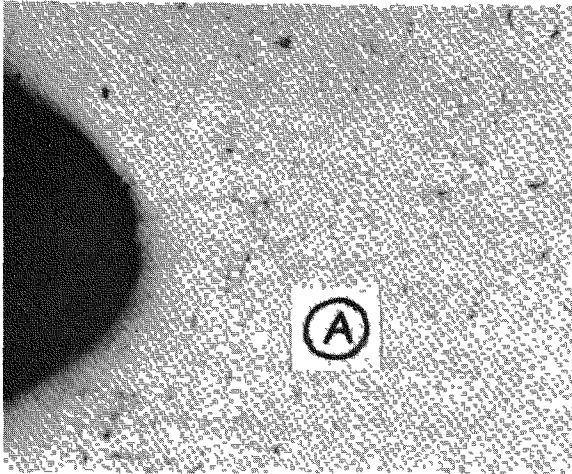
(a) No Load and P<1850 lb.

(b) P = 2000 lb.

FIGURE 14. Showing the Formation of a Crack in Front of the Notch Tip Prior to Reaching Maximum Load. The Observations were made on the Polished Surface after Unloading from the Indicated Loads. (Room Temperature Test; 200X Magnification). Continued.
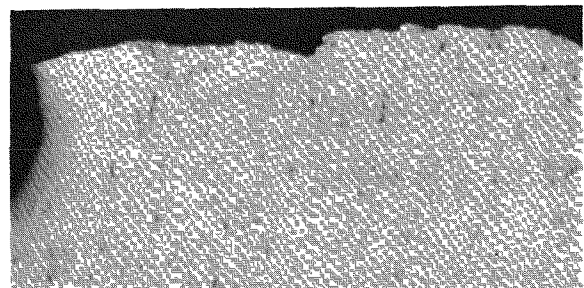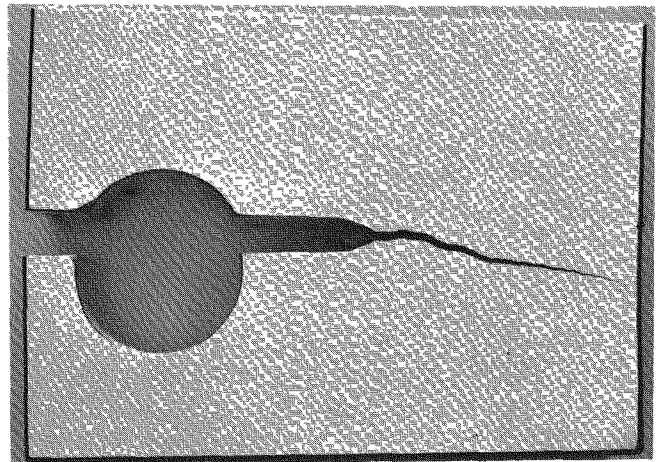
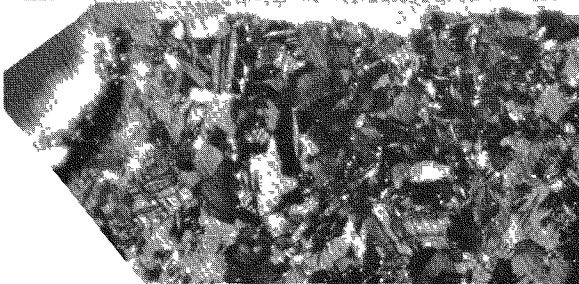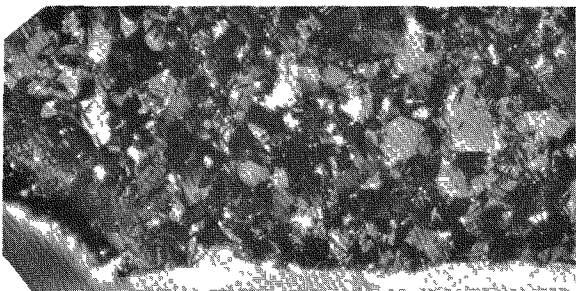(c) P = 2200 lb.

(d) Fracture, P = 2300 lb.

FIGURE 14. Continued

size but still considerably less than the 50 mil flat segment discussed above. Two other specimens were tested in a similar way. One showed no cracking or deformation of any sort prior to rupture. The other showed several cracks which formed at about 1900 lbs. at a position similar to that indicated by the circled A in Figure 14 (2200 lbs.). However, when final fracture occurred, neither of these cracks were part of the main fracture surface; in fact, they were quite far removed from the main fracture.

As was previously indicated, the grain structure and distribution of inclusions in the beryllium specimens can be seen in the micrographs of Figure 14. It might be noted, however, that the high density of twins observed in these micrographs was produced during metallographic polishing and are not present in the bulk material except near machined surfaces.

At the tip of the machined notches and side grooves there is a narrow zone for which the fracture appearance is like that shown in Figure 15a. This reflects the influence of the plastic deformation residual from machining operations. Just below this rim the cleavage facets have the usual appearance as shown in Figure 15b. This rim of slightly deformed material is due to the machining of the notches and is not due to shear lips normally associated with plane stress conditions at the surface. This is so because the distorted zone extends from the tip of the crack starting notches as well as along the sides of the specimens. Also, cleavage facets like those shown in Figure 15b extended right up to the edge of the notch and the sides of the specimen in the chemically etched and heat treated specimens. It is not believed that this machining induced deformation zone at the base of the notch had any influence on the K_{IC} test results.

Examples of the fracture appearance for both WOL and DCB type test specimens are shown in Figure 16. From visual or low magnification observations, the biggest difference in fracture appearance is noted between the heat treated and as-VHP conditions (see the WOL specimens in Figure 16). However, it is to be noted that if the specimens are examined at high magnification, the same features are observed (transcrystalline and grain boundary cleavage) in all the test specimens. The topography may vary, but the same cleavage facets
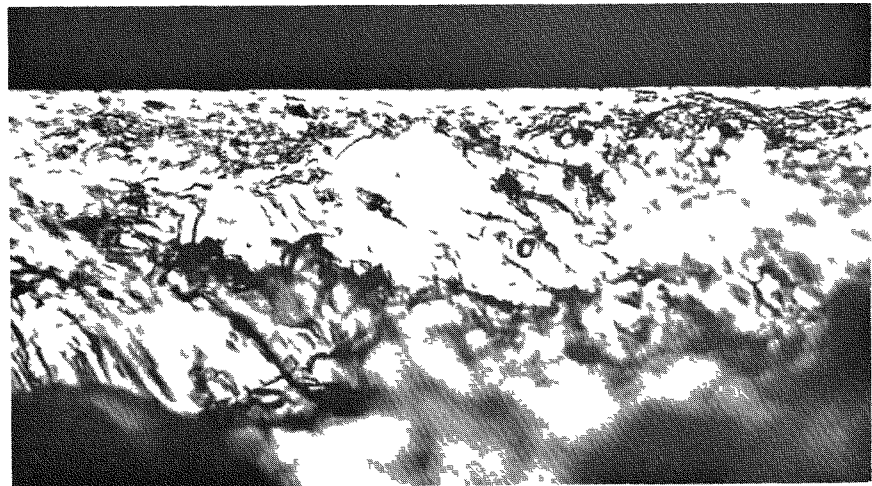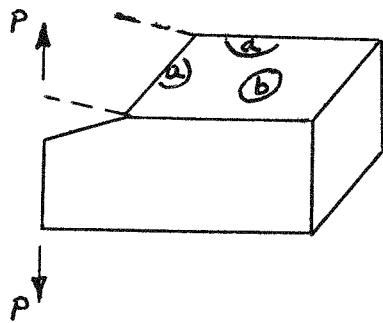
1500X

(a) Edge of Specimen and Tip of Notch
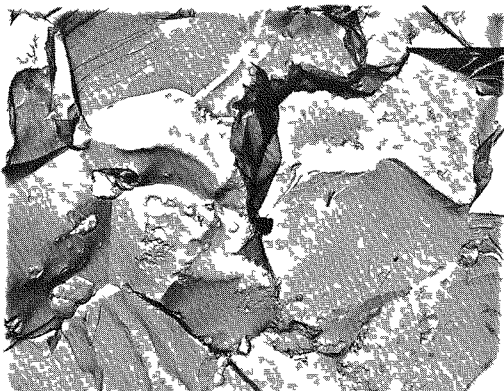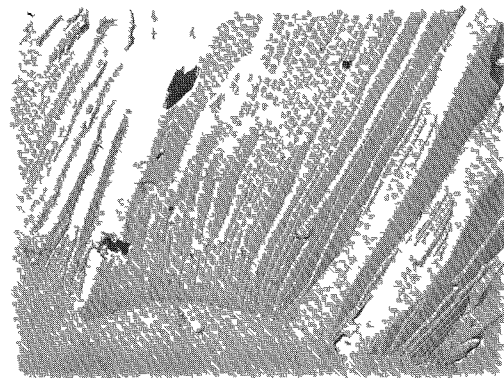
3000X   2500X

(b) Center of Specimen

FIGURE 15. Fractographs of Beryllium Specimen. (a) Optical Micrograph Showing
Machining-Induced Deformation Zone Near Surface. (b) Electron Micro-
graphs of Surface Replicas Taken near Center of Specimen. Schematic
at Upper Left Shows Locations of Micrographs.

31

(a)

75°F

-115°F

-320°F

(b)

L

L

T

75°F

-320°F

.005 in/min

2 in/min
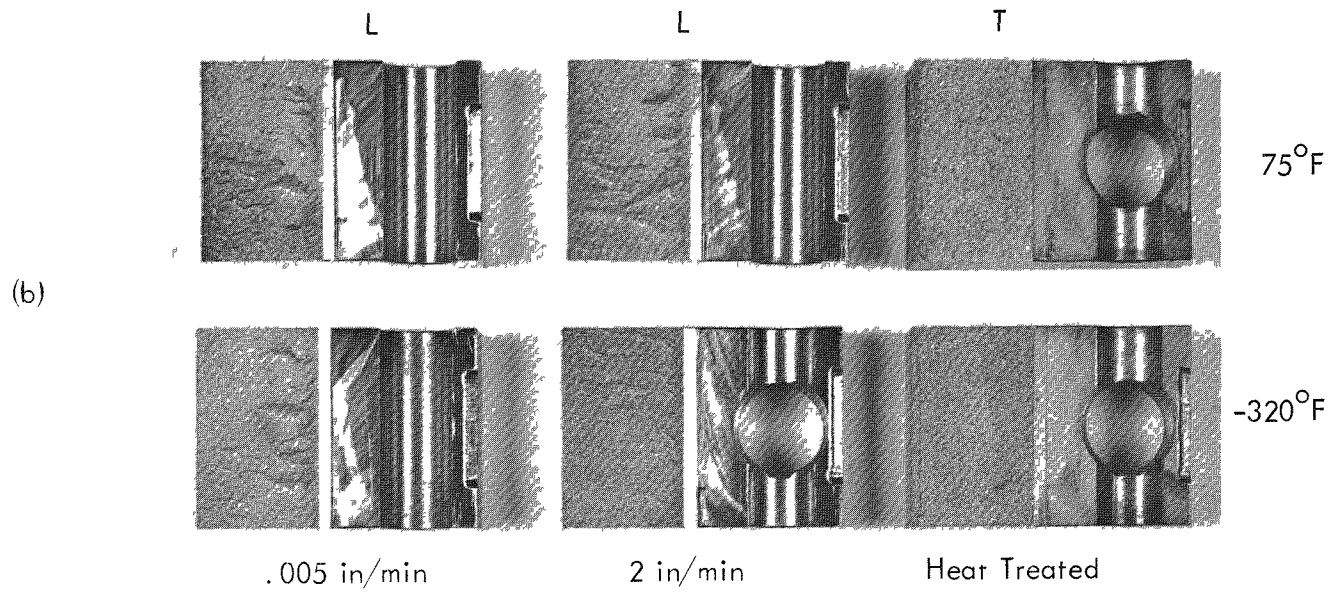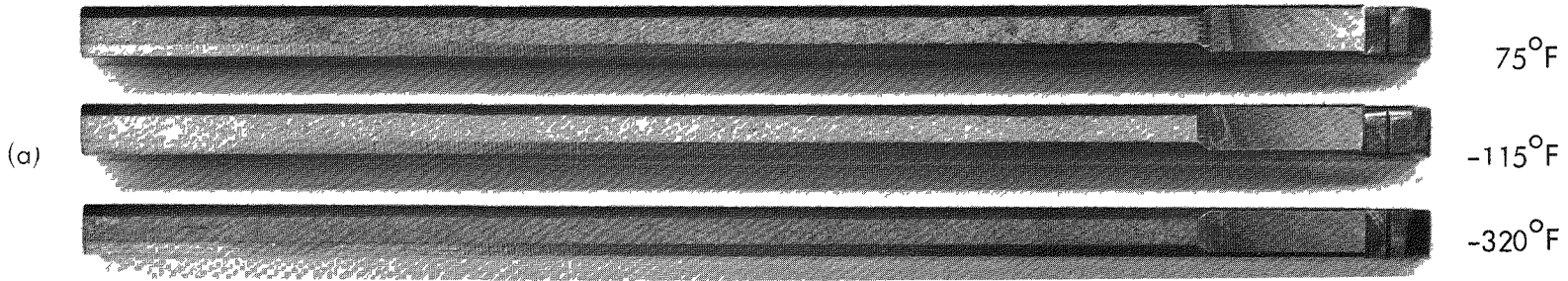
Heat Treated

FIGURE 16.   Fracture Surfaces of (a) DCB Specimens and (b) WOL Specimens

are seen in the as-VHP specimen tested at 500°F as are seen in the heat treated specimens tested at -320°F. Differences no doubt exist, but thus far they have not been detected even with surface replicas examined in the electron microscope.

DISCUSSION

SPECIMEN DESIGN

The K_{IC} values obtained with the WOL specimen are about 25-45% higher than those obtained with the DCB specimen, as shown by the summary curves in Figure 17. This, of course, raises a question as to which set of data, if either, is correct. Assessment of the validity of fracture toughness test results generally involves consideration of (1) the accuracy of the analytical expression used to calculate K_I (or G_I), (2) the degree to which the material behavior of the test specimen approximates linear elastic behavior during testing, and (3) the accuracy with which the relevant test parameters can be measured; e. g. , the load and crack length at the instant of instability. These factors have all been considered, and recognizing that there is no prior experience with beryllium to serve as a guide, the points discussed below have emerged as being of most significance.

The main point of contention with regard to the results obtained with the WOL specimen is whether or not the machined notch adequately simulated a natural crack. This question cannot be answered on theoretical grounds alone, and since the WOL specimens were not pre-cracked, the test results from this specimen alone are not sufficient for resolution of the question. However, it is recalled that a machined notch also existed during the first loading of the DCB specimens, and the value of G_{IC} obtained for the first loading was always in agreement with those obtained during subsequent loadings where natural cracks existed. In fact, the first value of G_{IC} was always lower than the average of the values obtained on a given test specimen. Thus, there is some basis for the view that the results obtained with the WOL specimen using the machined notches are valid.
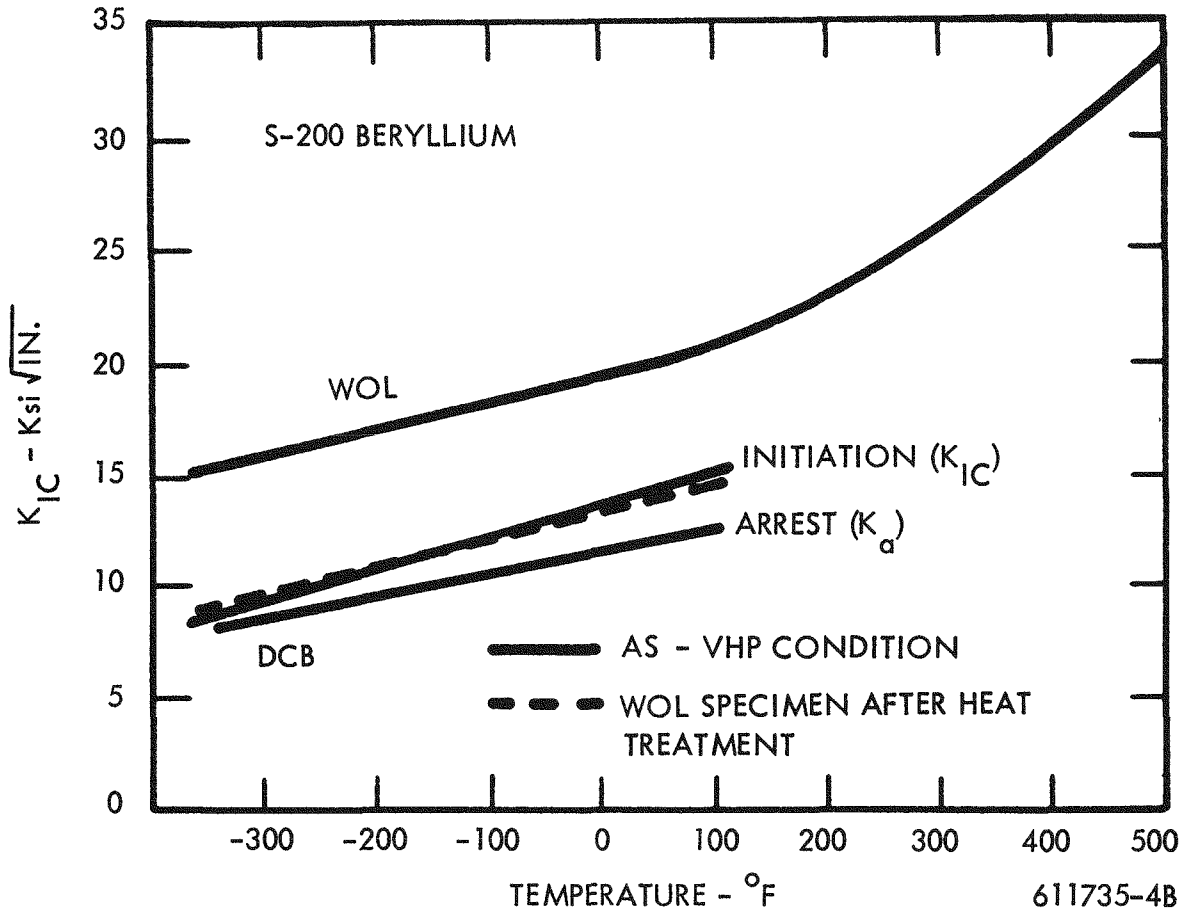
FIGURE 17. Summary of Fracture Toughness Data on Beryllium

There are several points of contention regarding the DCB specimen. The first concerns the accuracy of the K-calibration. In particular, the effect of the side grooves on the stress intensity factor is difficult to evaluate analytically. The method of calculating G_{IC} or K_{IC} employed in the present work was described in a previous section. Hoagland (Ref. 10) and Hoagland, Bement, and Rowe (Ref. 11) have evaluated the DCB specimen quite extensively and have determined the following expression on the basis of compliance measurements,

$$(\text{Eq. 10}) \qquad G_1 = \frac{ny^2 E}{2b_n A} \left[\frac{AP}{Ey}\right]^{\frac{n+1}{n}}$$

where n and A are constants for a given specimen geometry. The other symbols were defined in Figure 4. In terms of the compliance $C = Y/P$, this equation can be rewritten as

$$(\text{Eq. 11}) \qquad \frac{G}{P^2} = \frac{n}{2b_n} C^{2-\frac{(n+1)}{n}} E^{1-(\frac{n+1}{n})} A^{\frac{(n+1)}{n}-1}$$

For the specimen dimensions employed in the present work, Hoagland's values for n and A are n = 2.726 and A = 510. Using values of C and the associated crack lengths previously plotted in Figure 5 (Curve 4), Hoagland's equation gives the results shown by the solid circles in Figure 7. This agreement is quite good and lends credence to the present calculations since Hoagland supported his analysis with extensive testing.

One difficulty encountered with the DCB specimen was that of determining the compliance of the specimen during testing. An inherent feature of this specimen design, of course, is its high compliance which facilitates measurements. However, a number of the load-deflection curves were nonlinear and this rendered the compliance measurements somewhat subjective. This uncertainty as to the appropriate compliance to use for some of the curves was not of sufficient magnitude to account for the different results obtained with the DCB and WOL type specimens.

The tearing mode of failure observed in some of the tests, particularly for the heat treated specimens, was previously described and illustrated in Figure 12. This effect may be related

to an observation made by Hoagland. He found that for certain specimen dimensions a twisting type of elastic buckling occurred which subjected the crack tip to a shearing action, i.e., a mode III crack displacement. This elastic instability tends to decrease the apparent K_{IC} since an increase in the mode III stress field decreases the required opening mode stress field for crack propagation. This effect, which can be eliminated by increasing the specimen thickness, could have been present in all of the tests, and, if so, would have led to fictitiously low values of K_{IC}.

CRACK ARREST

In addition to providing measurements on the critical strain energy release rate for crack propagation, the DCB specimen also yields data on crack arrest; i.e., G_a. Whereas G_{IC} is a materials property independent of specimen dimensions and loading arrangement, G_a is not. Thus, the values of G_a depend upon kinetic energy considerations which vary with the test procedures as well as the properties of the material. The crack arrest values, therefore, should be viewed in a qualitative sense.

As discussed by Hoagland et al., the parameter G_a can be viewed as a qualitative measure of the ability of the material to arrest a rapidly propagating crack. Thus, the higher the value of G_a relative to G_{IC}, or equivalently the lower the value of $(G_{IC} - G_a)$, the less the crack will extend before it is arrested. The values of $(G_{IC} - G_a)$ for the beryllium specimens increased with increasing temperature, suggesting that the temperature dependence of G_{IC} is greater than that of G_a. Thus, once initiated, a crack would propagate a greater distance under fixed grip conditions the higher the temperature.

ANISOTROPY

The results obtained with the WOL specimen showed that the K_{IC} values obtained for the transverse specimens tended to be slightly higher than those for the longitudinal specimens. Also, as was shown in Figure 13, the fracture path for some of the transverse specimens tested at room temperature and at $500°F$ veered to the side of the specimen; i.e., the fracture

path changed to that characteristic of the longitudinal specimen orientation. (Note that the actual plane of the crack changed from a longitudinal to a transverse plane in the pressing.) Since the crack always extended a short distance in the plane of the notch before it changed direction, it is believed that the K_{IC} data are valid regardless of what happens after the onset of rapid fracture. It thus appears that specimen orientation has only a slight effect on the fracture toughness of this grade of beryllium. On the other hand, the fact that a definite, even though slight, effect of orientation was observed, suggests that anisotropy of fracture toughness might be quite pronounced in other less isotropic forms of beryllium.

HEAT TREATMENT

As judged by the results obtained with the WOL specimen, the fracture toughness of this grade of beryllium is markedly influenced by heat treatment. Although valid test data were not obtained with the heat treated DCB specimens, the pronounced difference in behavior between the as-VHP and heat treated specimens itself attests to the influence of heat treatment. The decrease in K_{IC} following heat treatment was about the same for all of the heat treat conditions studied. Preliminary optical metallographic studies failed to reveal any microstructural differences between the heat treated and initially as-VHP conditions.

FRACTURE APPEARANCE CRITERIA

In fracture toughness testing in general, it has been found useful to correlate transitions in toughness associated with variations in specimen dimensions or test temperature with transitions in fracture appearance. In extreme conditions, for example, square (flat) fractures with zero shear lips are associated with minimum plane strain K_{IC} values, and 100% slant (shear) fracture surfaces are associated with maximum plane stress toughness. Thus, the absence of shear lips is taken as an indication that plane strain conditions prevailed. Since no shear lips were observed on any of the beryllium specimens, it might be surmised that plane strain conditions existed for both the WOL and DCB type specimens. However, it is the author's experience with this grade of beryllium that fracture will occur by transcrystalline and intercrystalline cleavage even if preceeded by considerable plastic deformation.

Shear lips probably would not develop even in quite thin specimens. Consequently, fracture appearance criteria in assessing plane strain conditions appears to be of limited utility in the case of the metal beryllium.

CONCLUSIONS

The general level of magnitude of the opening mode plane strain fracture toughness, K_{IC}, of VHP S-200 beryllium was determined using two different test specimens in the temperature range -320 to 500°F. A number of other variables were also considered to a limited extent in order to gain a preliminary assessment of their possible effect on fracture toughness. The main results and conclusions from this study are the following:

1. Based upon the WOL test specimen, the measured value of K_{IC} was about 20Ksi $\sqrt{in}$ at room temperature and about 16 Ksi $\sqrt{in}$ at -320°F. The results with the DCB specimen were about 6 Ksi $\sqrt{in}$ lower than those from the WOL specimen throughout the temperature range studied.

2. The temperature dependence of K_{IC} was approximately linear in the range -320°F to 75°F. The rate of increase in K_{IC} with temperature above room temperature appears to be more rapid, as judged by one test at 500°F.

3. This particular form and grade of beryllium is approximately isotropic (within ~10%) with respect to fracture toughness. The slight anisotropy observed is in the direction of higher fracture toughness for specimens loaded in the transverse direction.

4. The fracture toughness does not appear to be very sensitive to the loading rate in the range 0.005 - 2.0 in/min crosshead speed.

5. The fracture toughness of the form and grade of beryllium studied is very sensitive to heat treatment. No gross microstructural nor fractographic features could be found to correlate with heat treatment. The effect of heat treatment should be studied in more detail. Fracture toughness may prove to be a sensitive tool for evaluating alloying and thermal-mechanical effects. Also, in many applications thermal treatments are employed in connection with stress relieving and brazing

processes, and the consequence of these thermal treatments on fracture toughness must be considered.

6. Caution must be used when employing fracture appearance criteria to assess plane strain conditions in the metal beryllium.

7. The crack arrest data obtained with the DCB specimen suggests that the ability of beryllium to arrest a crack is quite good.

8. Both of the test specimens employed in the present study show considerable promise for use in fracture mechanics studies on beryllium. However, additional research is needed to optimize specimen design and test procedures.

ACKNOWLEDGEMENTS

REFERENCES

1.   Harris, D. O. and Dunegan, H. L., "Fracture Toughness of Beryllium", Lawrence
        Radiation Laboratory, Report UCRL-70255, Preprint, January, 1967.

2.   Wilson, W. K., (Westinghouse Research Laboratories), Private Communication.

3.   Wessel, E. T., Clark, W. G., and Wilson, W. K., "Engineering Methods for the Design
        and Selection of Materials Against Fracture", Final Technical Report to U. S. Army
        Tank-Automotive Center, Contract No. DA-30-069-AMC-602(T), June, 1966.

4.   Wilson, W. K., "Review of Analysis and Development of WOL Specimen", Westinghouse
        Research Laboratories, Research Report 67-707-BTLPV-R1, March, 1967.

5.   See, for example, the paper by Srawley , J. E. and Brown, W. F., p. 160, in Fracture
        Toughness Testing and Its Application, ASTM-STP No. 381, (1965).

6.   Ripling, E. S., Mostovoy, S., and Patrick, R. L., "Measuring Fracture Toughness of
        Adhesive Joints", Materials Research and Standards, 4, No. 3, March, 1964, ASTM.

7.   Mostovoy, S., Crosely, P. B., and Ripling, E. J., "Use of Crack Lone Loaded Specimens
        for Measuring Plane Strain Fracture Toughness", Materials Research Laboratory, Inc.
        June, 1966. Paper Reprinted for the 3rd Annual Fracture Mechanics Summer Series, 1966.

8.   Bonfield, W. and Li, C. H., "The Microstrain Characteristics of Beryllium", Beryllium
        Technology, Vol. 1, 1. 539, Metallurgical Society Conference, Vol 33, AIME,
        Philadelphia, October 15-17, 1964, Gordon and Breach, 1966.

9.   Hanes, H. D., et. al., "Physical Metallurgy of Beryllium", DMIC Report 230, June,
        1966.

10.   Hoagland, R. G., "On the Use of the Double Cantilever Beam Specimen for Determining
        the Plane Strain Fracture Toughness of Metals", J. of Basic Engineering, Trans. ASME,
        Paper N, 67-Met-A.

11.   Hoagland, R. G., Bement, A. L, and Rowe, R. G., "Applications of Fracture Mechanics
        in Evaluating the Initiation and Propagation of Brittle Fracture in Reactor Structural
        Components", BNWL-SA-377, March, 1966.